Automatica 134 (2021) 109934

Contents lists available at ScienceDirect

Automatica

journal homepage: www.elsevier.com/locate/automatica

Safe convex-circumnavigation of one agent around multiple targets using bearing-only measurements[☆]

Shida Cao[a], Rui Li[a,*], Yingjing Shi[a], Yongduan Song[b,c]

[a] School of Automation Engineering, University of Electronic Science and Technology of China, Chengdu 611731, PR China
[b] Key Laboratory of Dependable Service Computing in Cyber Physical Society of Ministry of Education, Chongqing University, Chongqing 400044, PR China
[c] School of Automation, Chongqing University, Chongqing 400044, PR China

ARTICLE INFO

Article history:
Received 7 August 2020
Received in revised form 17 May 2021
Accepted 3 August 2021
Available online 11 October 2021

Keywords:
Multi-agent systems
Localization
Safe circumnavigation
Bearing measurements
Target estimator
Control protocol
Convex hull

ABSTRACT

This paper presents a new circumnavigation pattern — safe convex-circumnavigation, for the agent to enclose the targets closely, which is a pattern with better performance in harsh environments than the traditional circular circumnavigation pattern. With this new pattern, the agent circumnavigates the convex hull of multiple stationary targets with an expected enclosing distance and speed using the agent's known position as well as the bearing-only information of the targets, in addition, no collision with this convex hull happens in the whole time domain. An algorithm containing scalar estimators and a control protocol is proposed to implement this pattern. The estimators are designed to locate the targets. In the control protocol, the velocity of the agent is decomposed to one directly pointing to the convex hull and one orthogonal to its current direction. The agent is forced to circumnavigate the convex hull of the targets' estimated positions and finally circumnavigate the convex hull of the real targets because the estimators converge to the exact positions of the targets. The corresponding convergence analysis is provided subsequently. Numerical simulation and real time experiment are conducted to verify the proposed method.

1. Introduction

In recent years, the circumnavigation problems have attracted much attention of many research groups. The whole circumnavigation task can be divided into two phases: localization and circumnavigation. In some researches, the localization task can be accomplished easily since it is assumed that the agent's sensors can obtain the position information of the targets immediately (Franchi et al., 2016; Kim & Sugie, 2007; Lan et al., 2010; Li et al., 2016; Miao et al., 2017; Shames et al., 2011; Shi et al., 2015). However, sometimes the full position information of the targets may become unaccessible. Therefore, it needs to be further studied how the agent can perform circumnavigation with incomplete position information of the targets.

Incomplete position information is mainly divided into two types: distance-only (Cao, 2014, 2015; Hashemi et al., 2014; Matveev & Semakova, 2017; Matveev et al., 2016; Milutinović et al., 2017; Shames et al., 2012) and bearing-only information (Cao et al., 2020; Chun & Tian, 2020; Deghat et al., 2012, 2010, 2014, 2015; Dou et al., 2020; Li et al., 2018, 2019; Qi et al., 2019; Yu et al., 2019; Zheng et al., 2015). In this paper, we focus on bearing-only information. Bearing-only circumnavigation can be applied in many scenarios. For example, sometimes the working condition is so special that the agent must keep radio silence to avoid being detected by the hostile radars.

Much efforts have been made to solve such bearing-only circumnavigation problems. As a pioneering work, Deghat et al. (2010) investigate the case where one agent circumnavigates one static or moving target. It provides a very useful idea that the deviation can be constructed by an orthogonal projection method, which is widely adopted by others' following works. Deghat et al. (2015) is a multi-target generalization of this pioneering single-target work. Shao and Tian (2018) provide a multi-agent solution for the multi-target circumnavigation problem, in which a kind of consensus method is applied to the circumnavigation research area.

A point tends to be ignored that, in the previous works, they constrain the meaning of the word "circumnavigation" to "circular circumnavigation", which is only one pattern but should not

☆ This work is supported in part by the National Natural Science Foundation of China under Grant (Nos. 61973055, 61860206008, 61773081, 61933012, 61833013, 61991403, 61803053) and the Fundamental Research Funds for the Central Universities (No. ZYGX2019J062). The material in this paper was not presented at any conference. This paper was recommended for publication in revised form by Associate Editor Angelo Alessandri under the direction of Editor Thomas Parisini.

* Corresponding author.
E-mail addresses: lirui@uestc.edu.cn (S. Cao), lirui@uestc.edu.cn (R. Li), shiyingjing@uestc.edu.cn (Y. Shi), ydsong@cqu.edu.cn (Y. Song).

https://doi.org/10.1016/j.automatica.2021.109934
0005-1098/

be its entire meaning. In practice, the circumnavigation pattern matters if the environment or the circumnavigation objective changes. A recent work (Chun & Tian, 2020) proposes elliptical circumnavigation where new circumnavigation patterns other than circular ones are put forward. This work inspires us that, although circular circumnavigation is easy both to model and to solve, it is a rough pattern.

Based on the analysis above, it is discovered that to improve the circumnavigation performance, the "close" property should be paid more attention to. For a strip target shape, the elliptical circumnavigation is more "closer" than the circular one. However, it is still with low degrees of freedom because only the long and short axes can be specified. This leads us to think deeply about the exact meaning of the word "close". One can easily find that the convex hull of all the targets is an appropriate model to describe this area. Therefore, the objective of multi-target circumnavigation should be to enclose the convex hull as close as possible. This new circumnavigation pattern fits in harsh scenarios. For example, after earthquake, there may be an irregularly shaped area to be rescued and a quadrotor is ordered to enclose this area closely, so that the wounded people and the collapse areas can be detected more thoroughly.

Moreover, safety is another important issue. Safety means to avoid collision. Deghat et al. (2010) do not provide an idea for collision-avoidance because the initial position of the estimate can greatly affect the movement of the agent, thus collision may happen in the initial phase of the estimator's convergence process. Li et al. (2019) use estimators similar to that of Deghat et al. (2010) and collision is avoided by constraining the initial positions of the estimates of the targets to an area near to the real targets, which is a strict condition. In our previous work (Cao et al., 2020), a new scalar estimator is designed and it provides a mechanism for collision-avoidance with a loose initial condition. However, that paper does not take the multi-target scenario into consideration.

Inspired by the aforementioned works, in this paper, we study the safe convex-circumnavigation problem, in which the agent safely circumnavigates the convex hull of all the targets with a desired distance and speed using the bearing-only information. We aim to develop estimators for targets localization and a control protocol for convex-circumnavigation. The estimation method in Cao et al. (2020) is adopted and it is improved by adding a sign term to fit in the multi-target scenario. Furthermore, to drive the agent to move around the convex hull of all the targets, unlike in the existing works, in this paper, a control protocol is designed in which the agent's velocity is decomposed into the direction pointing to the convex hull and its orthogonal direction. In addition, safety is also guaranteed.

The main contributions of this work are threefold.

(1) A novel circumnavigation pattern — safe convex-circumnavigation is proposed. With this pattern, the agent encloses all the targets more closely than with the circular pattern. Thus the circumnavigation can be done in harsher environments and the targets are detected more thoroughly.
(2) A control protocol is designed for the safe convex-circumnavigation problem using bearing-only information of the targets, with which the safety is guaranteed in the whole circumnavigation process. Meanwhile, the initial conditions are as loose as in Cao et al. (2020) although multiple targets are considered.
(3) Compared with previous multi-target papers (Chun & Tian, 2020; Deghat et al., 2015; Li et al., 2019), with our algorithm one just needs to specify the desired distance from the agent to the convex hull of the targets. No desired distance related to the center of the targets needs to be preset.

The rest of this paper is structured as follows. In Section 2, mathematical preliminaries are introduced and the safe convex-circumnavigation problem is formally stated. Then we propose an algorithm to solve this problem and prove the convergence property of it in Section 3. Simulations are conducted in Section 4. Discussion about moving targets case is given in Section 5, in which an experiment is done to show the feasibility of our algorithm when targets move. Conclusions are demonstrated in Section 6.

2. Preliminaries and problem statement

2.1. Mathematical preliminaries and notations

Suppose there is a multi-agent system composed of an agent and n stationary targets. Denote the targets by $\mu_1, \ \mu_2, \ \ldots, \ \mu_n$ to distinguish them. In the system, the agent can measure its own position as well as the bearing angle from itself to each target, while the distance information from the agent to each target is unavailable. It is supposed that the agent is with single integrator dynamics, i.e., the velocity of the agent can be directly controlled.

2.1.1. Basic notations

Firstly, we introduce some general mathematical notations: $\mathbb{Z}$ is the set of integers. $\mathbb{R}$ is the set of real numbers. $\mathbb{R}_{\geq 0}$ is the set of non-negative real numbers. $\mathbb{R}_+$ is the set of positive real numbers. $\mathbb{R}^2$ is the set of 2D column vectors. $\mathbf{0}$ is the ordinary point of $\mathbb{R}^2$. $\boldsymbol{I}$ is the 2×2 identity matrix. $\|\cdot\|$ is the Euclidean norm. $\mathbb{S}^1$ is the set of unit vectors, $\mathbb{S}^1 \triangleq \{\boldsymbol{u} \in \mathbb{R}^2 \mid \|\boldsymbol{u}\| = 1\}$. For two unit vectors $\boldsymbol{u}, \boldsymbol{v} \in \mathbb{S}^1$, $\langle \boldsymbol{u}, \boldsymbol{v} \rangle$ is the angle between them, and it is noticeable that $\langle \boldsymbol{u}, \boldsymbol{v} \rangle \in [0, \pi]$. For a set A, $|A|$ is the cardinality of it. For two sets A and B, $A \setminus B \triangleq \{x \mid x \in A \text{ and } x \notin B\}$ represents the difference of them. If the elements of a finite set are with ordered indices, for example, $A = \{a_1, a_2, \ldots, a_m\}$, then we use a compact form $A = \{a_i\}_{i=1}^n$ to represent this set. For a function $f : \mathbb{R}^2 \to \mathbb{R}$, ∇f is the gradient of it and is viewed as a column vector. If $g(t)$ is a scalar- or vector-valued function of the time t, then $\dot{g}(t)$ denotes the derivative of g over t. For a function $h(t)$ over the time t, $h : \mathbb{R}_{\geq 0} \to A$, we use $h(t) \in A$ to represent that the codomain of $h(t)$ is A.

Some basic concepts associated with the circumnavigation problem are defined as below.

Notation 1. *Several concepts need to be defined:*

$\boldsymbol{y}(t) \in \mathbb{R}^2$	*The position of the agent*
$\boldsymbol{x}_i \in \mathbb{R}^2$	*The position of the stationary target* μ_i
$X \subset \mathbb{R}^2$	*The set of positions of all of the targets,* $X \triangleq \{\boldsymbol{x}_i\}_{i=1}^n$
$\rho_i(t) \in \mathbb{R}_{\geq 0}$	*The distance between the agent and the target* μ_i, $\rho_i(t) \triangleq \|\boldsymbol{x}_i - \boldsymbol{y}(t)\|$
$\boldsymbol{\varphi}_i(t) \in \mathbb{S}^1$	*The unit vector from the agent to the target* μ_i, $\boldsymbol{\varphi}_i(t) \triangleq [\boldsymbol{x}_i - \boldsymbol{y}(t)]/\rho_i(t)$ *(if* $\rho_i(t) > 0$*)*
$\Phi(t) \subset \mathbb{S}^1$	*The set of unit vectors from the agent to the targets at time* t, $\Phi(t) \triangleq \{\boldsymbol{\varphi}_i(t)\}_{i=1}^n$
$\bar{\boldsymbol{\varphi}}_i(t) \in \mathbb{S}^1$	$\boldsymbol{\varphi}_i(t)$ *rotates* $\pi/2$ *clockwise*
$\hat{\rho}_i(t) \in \mathbb{R}$	*The distance between the agent and the estimated position of the target* μ_i *along the direction of* $\boldsymbol{\varphi}_i(t)$
$\tilde{\rho}_i(t) \in \mathbb{R}$	*The estimation error of the distance between the agent and the target* μ_i, $\tilde{\rho}_i(t) \triangleq \hat{\rho}_i(t) - \rho_i(t)$
$\hat{\boldsymbol{x}}_i(t) \in \mathbb{R}^2$	*The estimated position of the target* μ_i, $\hat{\boldsymbol{x}}_i(t) \triangleq \boldsymbol{y}(t) + \hat{\rho}_i(t)\boldsymbol{\varphi}_i(t)$
$\hat{X}(t) \subset \mathbb{R}^2$	*The set of estimated positions of all of the targets at time* t, $\hat{X}(t) \triangleq \{\hat{\boldsymbol{x}}_i(t)\}_{i=1}^n$
$d \in \mathbb{R}_+$	*The expected enclosing distance*
$\alpha \in \mathbb{R}_+$	*The tangential enclosing speed*
$r_s \in \mathbb{R}_+$	*The safety distance*

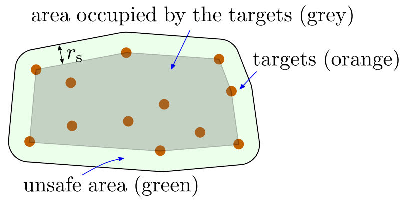

Fig. 1. The concept of safety.

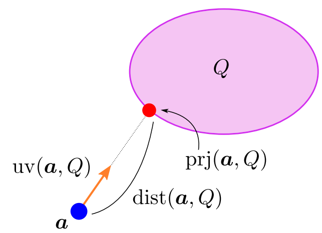

Fig. 2. Relationship between a point and a convex set.

Remark 2. At some time t', the elements of $\Phi(t')$ may be repeated. To avoid it, we introduce a convention that at each time t, the repeated elements are removed and $\Phi(t)$ contains each element only once.

2.1.2. Convex hull

It should be noted in particular that the concept of collision in this paper is unusual. In common sense, it is said that collision happens if the agent gets unsafely near to a certain target, technically speaking, if any ρ_i becomes less than the safety distance r_s. Nevertheless, if all of the targets are viewed as a whole, then the agent should not keep too close to the area occupied by the targets and should perform circumnavigation outside this area with a distance larger than r_s. See Fig. 1 for illustration. In the sequel, we clearly define this "area" as the convex hull of all of the targets and also define some concepts related to the convex hull. Thus, to prove that collision does not happen becomes to prove the distance between the agent and this convex hull is always larger than r_s. The formal definition of collision is also given in the following.

Definition 3 (*Convex Hull of Finite Point Sets*)**.** Suppose $P = \{\boldsymbol{p}_i\}_{i=1}^m$ is a subset of $\mathbb{R}^2$. We define $\mathrm{conv}(P)$ as the convex hull of P, such that $\mathrm{conv}(P) \triangleq \{\sum_{i=1}^m k_i \boldsymbol{p}_i \mid k_i \geq 0, i = 1, 2, \ldots, m, \sum_{i=1}^m k_i = 1\}$.

We present a basic proposition of convex sets (Boyd & Vandenberghe, 2004) as below, which provides a foundation for its next definition.

Proposition 4. *Suppose $Q \subset \mathbb{R}^2$ is compact and convex, $\boldsymbol{a} \in \mathbb{R}^2$ is a point. Then we can assert that there exists a unique point $\boldsymbol{b} \in Q$ such that $\|\boldsymbol{a} - \boldsymbol{b}\| = \inf_{\boldsymbol{q} \in Q} \|\boldsymbol{a} - \boldsymbol{q}\|$.*

Definition 5 (*Relationship Between a Point and a Convex Set*)**.** Suppose $Q \subset \mathbb{R}^2$ is a set and $\boldsymbol{a} \in \mathbb{R}^2$ is a point. Define $\mathrm{dist}(\boldsymbol{a}, Q)$ as the distance from $\boldsymbol{a}$ to Q, that is, $\mathrm{dist}(\boldsymbol{a}, Q) \triangleq \inf_{\boldsymbol{q} \in Q} \|\boldsymbol{a} - \boldsymbol{q}\|$. If Q is compact and convex, then we can define $\mathrm{prj}(\boldsymbol{a}, Q)$ as the minimum distance point in Q to $\boldsymbol{a}$, which satisfies that $\|\mathrm{prj}(\boldsymbol{a}, Q) - \boldsymbol{a}\| = \mathrm{dist}(\boldsymbol{a}, Q)$. If $\mathrm{dist}(\boldsymbol{a}, Q) > 0$, define $\mathrm{uv}(\boldsymbol{a}, Q)$ as the unit vector pointing from $\boldsymbol{a}$ to Q, i.e., $\mathrm{uv}(\boldsymbol{a}, Q) \triangleq [\mathrm{prj}(\boldsymbol{a}, Q) - \boldsymbol{a}]/\mathrm{dist}(\boldsymbol{a}, Q)$. See Fig. 2 for illustration.

With the concepts defined above, we then define some concepts associated with our safe convex-circumnavigation problem as below.

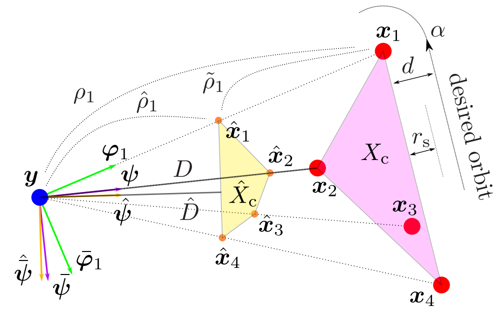

Fig. 3. Relationship among variables ($|X| = 4$).

Notation 6. *Define:*

$X_c \subset \mathbb{R}^2$	*The convex hull of all of the targets,* $X_c \triangleq \mathrm{conv}(X)$
$\hat{X}_c(t) \subset \mathbb{R}^2$	*The convex hull of all of the targets' estimates at time t,* $\hat{X}_c(t) \triangleq \mathrm{conv}(\hat{X}(t))$
$D(t) \in \mathbb{R}_{\geq 0}$	*The distance from the agent to the convex hull of all of the targets,* $D(t) \triangleq \mathrm{dist}(\boldsymbol{y}(t), X_c)$
$\hat{D}(t) \in \mathbb{R}_{\geq 0}$	*The distance from the agent to the convex hull of all of the targets' estimates,* $\hat{D}(t) \triangleq \mathrm{dist}(\boldsymbol{y}(t), \hat{X}_c(t))$
$\boldsymbol{\psi}(t) \in \mathbb{R}^2$	*The unit vector pointing from the agent to the convex hull of all of the targets,* $\boldsymbol{\psi}(t) \triangleq \mathrm{uv}(\boldsymbol{y}(t), X_c)$ *(if $D(t) > 0$)*
$\bar{\boldsymbol{\psi}}(t) \in \mathbb{R}^2$	$\boldsymbol{\psi}(t)$ *rotates $\pi/2$ clockwise*
$\hat{\boldsymbol{\psi}}(t) \in \mathbb{R}^2$	*The unit vector pointing from the agent to the convex hull of all of the targets' estimates,* $\hat{\boldsymbol{\psi}}(t) \triangleq \mathrm{uv}(\boldsymbol{y}(t), \hat{X}_c(t))$ *(if $\hat{D}(t) > 0$)*
$\bar{\hat{\boldsymbol{\psi}}}(t) \in \mathbb{R}^2$	$\hat{\boldsymbol{\psi}}(t)$ *rotates $\pi/2$ clockwise*

Variables in Notation 1 and 6 are shown in Fig. 3.

2.1.3. Angle notations

Moreover, sometimes we use radian angles to represent the direction of unit vectors. Define an equivalence relation $\sim$ in $\mathbb{R}$: $\beta \sim \beta_0 \iff \beta = \beta_0 + 2k\pi$ $(k \in \mathbb{Z})$. Denote $\mathbb{R}_{2\pi}$ as the equivalence class $\mathbb{R}/\sim$, which can be used to represent unit vectors. An element of $\mathbb{R}_{2\pi}$ is represented by $[\beta]$, in which $\beta \in \mathbb{R}$ is a representative. In $\mathbb{R}_{2\pi}$, the plus and minus operations are also well-defined such that $[\beta] \pm [\gamma] \triangleq [\beta \pm \gamma]$. Define $\angle : \mathbb{S}^1 \to \mathbb{R}_{2\pi}, \boldsymbol{u} = [\cos\beta, \sin\beta]^{\mathrm{T}} \mapsto \angle\boldsymbol{u} = [\beta]$. For $[\beta] \in \mathbb{R}_{2\pi}$, we denote $\arg([\beta]) \in [0, 2\pi)$ as the principal value. With this definition, for $\boldsymbol{u}, \boldsymbol{v} \in \mathbb{S}^1$, $\arg(\angle\boldsymbol{u} - \angle\boldsymbol{v})$ is the angle with which $\boldsymbol{v}$ rotates anticlockwise to $\boldsymbol{u}$.

As is shown in Fig. 3, the angle spanned by the unit vectors from the agent to the targets is like the visual angle of an eye. For an eye, the vision is limited and the leftmost and rightmost view can be modeled as two unit vectors. Inspired by this, we give the following definition to describe an aspect of the unit vectors from the agent to the targets.

Definition 7 (*Visual-angle Property*)**.** Suppose $V = \{\boldsymbol{v}_i\}_{i=1}^m$ is a subset of $\mathbb{S}^1$. We say the set V has visual-angle property if there exists $\boldsymbol{v}_r \in V$ such that $\arg(\angle\boldsymbol{v}_i - \angle\boldsymbol{v}_r) < \pi$ for $i = 1, 2, \ldots, m$. Then we define $\boldsymbol{v}_r$ as the rightmost unit vector of V and use the notation $\mathrm{ruv}(V)$ to represent it. For an element $\boldsymbol{v}_l \in V$, if there is $\langle \boldsymbol{v}_l, \boldsymbol{v}_r \rangle = \max_{1 \leq i \leq n} \langle \boldsymbol{v}_i, \boldsymbol{v}_r \rangle$, then we define $\boldsymbol{v}_l$ as the leftmost unit vector of V and use the notation $\mathrm{luv}(V)$ to represent it. In addition, define $\mathrm{ma}(V)$ as the maximum angle of V, that is, $\mathrm{ma}(V) \triangleq \langle \boldsymbol{v}_l, \boldsymbol{v}_r \rangle$. See Fig. 4.

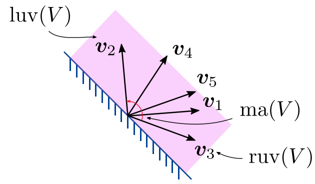

Fig. 4. Visual-angle property ($|V| = 5$).

In $\mathbb{R}_{2\pi}$, there are no natural order relations like in $\mathbb{R}$. But we need such a relation to describe the angle relationships. In the following, a kind of order relations is introduced into $\mathbb{R}_{2\pi}$ according to the rightmost unit vector of a set with visual-angle property.

Definition 8 (*Order Relation According to a Set with Visual-angle Property*)**.** Suppose $V = \{\boldsymbol{v}_i\}_{i=1}^m$ is a subset of $\mathbb{S}^1$ and has visual-angle property. Let $\boldsymbol{v}_\mathrm{r} \triangleq \mathrm{ruv}(V)$. According to V, we define $\leq$ as the order relation of less than or equal to and $<$ as the order relation of less than in $\mathbb{R}_{2\pi}$: (1) $[\beta] \leq [\gamma]$ iff $\arg([\beta] - \angle\boldsymbol{v}_\mathrm{r}) \leq \arg([\gamma] - \angle\boldsymbol{v}_\mathrm{r})$; (2) $[\beta] < [\gamma]$ iff $\arg([\beta] - \angle\boldsymbol{v}_\mathrm{r}) < \arg([\gamma] - \angle\boldsymbol{v}_\mathrm{r})$.

The below proposition gives a description of angle relationship of some kind of unit vectors and plays an important role to find the angle relationship among $\boldsymbol{\varphi}_i(t)$, $\boldsymbol{\psi}(t)$ and $\hat{\boldsymbol{\psi}}(t)$. Its proof is in Appendix.

Proposition 9. *Suppose $P = \{\boldsymbol{p}_i\}_{i=1}^m$ is a subset of $\mathbb{R}^2$. Let $P_\mathrm{c} \triangleq \mathrm{conv}(P)$, $\boldsymbol{a} \in \mathbb{R}^2 \setminus P_\mathrm{c}$, $\boldsymbol{v}_i \triangleq (\boldsymbol{p}_i - \boldsymbol{a})/\|\boldsymbol{p}_i - \boldsymbol{a}\|$ $(i = 1, 2, \ldots, m)$, $V \triangleq \{\boldsymbol{v}_i\}_{i=1}^m$, $\boldsymbol{u} \triangleq \mathrm{uv}(\boldsymbol{a}, P_\mathrm{c})$. Then V has visual-angle property. Let $\boldsymbol{v}_\mathrm{l} \triangleq \mathrm{luv}(V)$, $\boldsymbol{v}_\mathrm{r} \triangleq \mathrm{ruv}(V)$ and $\leq$ be the order relation of less than or equal to according to V. Then we can assert that (1) $\angle\boldsymbol{v}_\mathrm{r} \leq \angle\boldsymbol{u} \leq \angle\boldsymbol{v}_\mathrm{l}$; (2) $\langle\boldsymbol{u}, \boldsymbol{v}_i\rangle < \pi/2$ for $i = 1, 2, \ldots, m$.*

With Proposition 9, when $\boldsymbol{y}(t) \notin X_\mathrm{c}$, we know $\Phi(t)$ has visual-angle property at any time t. Then we are able to further define some concepts as below.

Notation 10. *When $\boldsymbol{y}(t) \notin X_\mathrm{c}$, define:*

$\boldsymbol{\varphi}_\mathrm{l}(t) \in \mathbb{S}^1$	*The leftmost unit vector of all of the unit vectors from the agent to the targets, $\boldsymbol{\varphi}_\mathrm{l}(t) \triangleq \mathrm{luv}(\Phi(t))$*
$\boldsymbol{\varphi}_\mathrm{r}(t) \in \mathbb{S}^1$	*The rightmost unit vector of all of the unit vectors from the agent to the targets, $\boldsymbol{\varphi}_\mathrm{r}(t) \triangleq \mathrm{ruv}(\Phi(t))$*
$\theta_\mathrm{m}(t) \in [0, \pi)$	*The maximum angle between the unit vectors from the agent to the targets, $\theta_\mathrm{m}(t) \triangleq \mathrm{ma}(\Phi(t))$*
$\leq_t$	*Order relation of less than or equal to according to $\Phi(t)$*
$<_t$	*Order relation of less than according to $\Phi(t)$*

2.2. Problem statements

In this subsection, we introduce some terms to facilitate our statements.

Definition 11 (*Localization*)**.** We say localization of all of the targets is achieved if $\lim_{t\to+\infty} \tilde{\rho}_i(t) = 0$ for $i = 1, 2, \ldots, n$.

Definition 12 (*Convex-circumnavigation*)**.** Suppose $P = \{\boldsymbol{p}_i\}_{i=1}^m$ is a subset of $\mathbb{R}^2$. Let $P_\mathrm{c} \triangleq \mathrm{conv}(P)$, $L(t) \triangleq \mathrm{dist}(\boldsymbol{y}(t), P_\mathrm{c})$, $\boldsymbol{\phi}(t) \triangleq \mathrm{uv}(\boldsymbol{y}(t), P_\mathrm{c})$, and $\bar{\boldsymbol{\phi}}(t)$ be the unit vector that $\boldsymbol{\phi}(t)$ rotates $\pi/2$ clockwise. The agent is said to perform convex-circumnavigation around P with the radius d and the speed α if the following two conditions hold: (1) $\lim_{t\to+\infty} L(t) = d$; (2) $\lim_{t\to+\infty} \bar{\boldsymbol{\phi}}^\mathrm{T}(t)\dot{\boldsymbol{y}}(t) = \alpha$.

Remark 13. When we say that the agent performs convex-circumnavigation around all of the targets, we mean that the agent performs convex-circumnavigation around X.

Definition 14 (*Collision*)**.** We say collision happens at time t' if $D(t') < r_\mathrm{s}$.

Definition 15 (*Safe*)**.** We say a circumnavigation algorithm is safe if collision never happens in the whole time domain $\mathbb{R}_{\geq 0}$.

In this paper, we assume that only the bearing information can be accessed, so the exact position of each target is unknown in the beginning. We should first make efforts to estimate each target's position to locate them. Therefore, besides a control protocol to drive the agent to move around the targets, estimators that converge to the targets' exact positions should also be designed.

Now we are ready to give a formal statement of the problem of safe convex-circumnavigation.

Problem 16. Consider a 2D multi-agent system containing a group of stationary targets and a single agent with the first-order integrator dynamics. The agent can locate itself but can only access the bearing information from itself to the targets. The objectives of the safe convex-circumnavigation problem include:

(1) Localization of all of the targets should be achieved. An estimation method should be designed to find out the exact position of all of the targets.
(2) Convex-circumnavigation around all of the targets should be performed. A control protocol should be developed to drive the agent into a steady state, in which it encloses all of the targets with the desired distance and speed in the end.
(3) Safety should be guaranteed. Collision should be avoided during the whole circumnavigating process.

3. Main results

In this section, we present an algorithm consisting of estimators and a control protocol to solve the safe convex-circumnavigation problem. Then the convergence analysis is presented.

3.1. Proposed algorithm

In this subsection, we provide a solution for the safe convex-circumnavigation problem. We first make efforts to estimate the position of each target to make it possible to perform circumnavigation tasks around the real targets. In this paper, the distance from the agent to each target is estimated and the estimators are

$$\dot{\hat{\rho}}_i(t) = -\boldsymbol{\varphi}_i^\mathrm{T}(t)\dot{\boldsymbol{y}}(t) + \mathrm{sgn}(\bar{\boldsymbol{\varphi}}_i^\mathrm{T}(t)\dot{\boldsymbol{y}}(t))\bar{\boldsymbol{\varphi}}_i^\mathrm{T}(t)\dot{\hat{\boldsymbol{x}}}_i(t). \tag{1}$$

Here, $\mathrm{sgn}(\cdot)$ is the sign function.

Subsequently, the control protocol is

$$\dot{\boldsymbol{y}}(t) = k[\hat{D}(t) - d]\hat{\boldsymbol{\psi}}(t) + \alpha u(\hat{D}(t) - r_\mathrm{s})\bar{\hat{\boldsymbol{\psi}}}(t). \tag{2}$$

Here, $u(\cdot)$ is the step function.

Now we are in the position to state the assumptions, which are weak and easy to guarantee in practice. The first assumption means that collision does not happen in the beginning. The second assumption means that the expected enclosing distance is larger than the safe distance. The third assumption is a constraint on the initial value of the estimate of each target and it is loose since we can just set $\hat{\rho}_i(0)$ to r_s.

Assumption 17. $D(0) \geq r_\mathrm{s}$.

Assumption 18. $d > r_{\rm s}$.

Assumption 19. $r_{\rm s} \le \hat{\rho}_i(0) \le \rho_i(0)$ for $i = 1, 2, \ldots, n$.

3.2. Convergence analysis

In this subsection, we prove the convergence property of the proposed method. Safety property is verified at first, and then we prove that the agent eventually performs safe convex-circumnavigation around all of the targets successfully.

3.2.1. Safety

In this subsection, most of the efforts are taken to verify that collision does not happen in the whole time domain. Additionally, we also prove the boundedness of $D(t)$.

Denote $v_i(t) \triangleq \boldsymbol{\varphi}_i^{\rm T}(t)\dot{\boldsymbol{y}}(t)$, $\bar{v}_i(t) \triangleq \bar{\boldsymbol{\varphi}}_i^{\rm T}(t)\dot{\boldsymbol{y}}(t)$, $\omega_i(t) \triangleq \bar{v}_i(t)/\rho_i(t)$. Omitting "$(t)$", it follows that

$$\dot{\boldsymbol{\varphi}}_i = \frac{\mathrm{d}}{\mathrm{d}t}\frac{\boldsymbol{x}_i - \boldsymbol{y}}{\|\boldsymbol{x}_i - \boldsymbol{y}\|} = \frac{\left(\boldsymbol{I} - \boldsymbol{\varphi}_i\boldsymbol{\varphi}_i^{\rm T}\right)(\dot{\boldsymbol{x}}_i - \dot{\boldsymbol{y}})}{\|\boldsymbol{x}_i - \boldsymbol{y}\|}$$

$$= -\frac{\bar{\boldsymbol{\varphi}}_i\bar{\boldsymbol{\varphi}}_i^{\rm T}\dot{\boldsymbol{y}}}{\|\boldsymbol{x}_i - \boldsymbol{y}\|} = -\frac{\bar{v}_i}{\rho_i}\bar{\boldsymbol{\varphi}}_i = -\omega_i\bar{\boldsymbol{\varphi}}_i, \tag{3}$$

$$\dot{\hat{\boldsymbol{x}}}_i = \frac{\mathrm{d}}{\mathrm{d}t}(\boldsymbol{y} + \hat{\rho}_i\boldsymbol{\varphi}_i) = \dot{\boldsymbol{y}} + \dot{\hat{\rho}}_i\boldsymbol{\varphi}_i + \hat{\rho}_i\dot{\boldsymbol{\varphi}}_i,$$

$$\dot{\hat{\rho}}_i = -\boldsymbol{\varphi}_i^{\rm T}\dot{\boldsymbol{y}} + \mathrm{sgn}(\bar{\boldsymbol{\varphi}}_i^{\rm T}\dot{\boldsymbol{y}})\bar{\boldsymbol{\varphi}}_i^{\rm T}\dot{\hat{\boldsymbol{x}}}_i = -v_i - |\bar{v}_i|\frac{\tilde{\rho}_i}{\rho_i}, \tag{4}$$

$$\dot{\rho}_i = \frac{\mathrm{d}}{\mathrm{d}t}\|\boldsymbol{x}_i - \boldsymbol{y}\| = -v_i,$$

$$\dot{\tilde{\rho}}_i = \dot{\hat{\rho}}_i - \dot{\rho}_i = -\frac{|\bar{v}_i|}{\rho_i}\tilde{\rho}_i = -|\omega_i|\tilde{\rho}_i. \tag{5}$$

Firstly, angle relation among unit vectors is revealed.

Lemma 20. *If $D(t) > 0$ and $\hat{D}(t) > 0$, then it is true that $\boldsymbol{\psi}^{\rm T}(t)\hat{\boldsymbol{\psi}}(t) > 0$ and $\boldsymbol{\varphi}_i^{\rm T}(t)\hat{\boldsymbol{\psi}}(t) > 0$ for $i = 1, 2, \ldots, n$.*

Proof. With Proposition 9, it is obvious that $\boldsymbol{\varphi}_i^{\rm T}(t)\hat{\boldsymbol{\psi}}(t) > 0$ holds at any time t for $i = 1, 2, \ldots, n$. So we only prove $\boldsymbol{\psi}^{\rm T}(t)\hat{\boldsymbol{\psi}}(t) > 0$. Using Proposition 9 again, we know

(1) If $0 \le \theta_{\rm m}(t) < \pi/2$, then

$$\angle\boldsymbol{\varphi}_{\rm r}(t) \le_t \angle\boldsymbol{\psi}(t) \le_t \angle\boldsymbol{\varphi}_{\rm l}(t),$$
$$\angle\boldsymbol{\varphi}_{\rm r}(t) \le_t \angle\hat{\boldsymbol{\psi}}(t) \le_t \angle\boldsymbol{\varphi}_{\rm l}(t).$$

(2) If $\pi/2 \le \theta_{\rm m}(t) < \pi$, then

$$\angle\boldsymbol{\varphi}_{\rm l}(t) - \left[\frac{\pi}{2}\right] <_t \angle\boldsymbol{\psi}(t) <_t \angle\boldsymbol{\varphi}_{\rm r}(t) + \left[\frac{\pi}{2}\right],$$
$$\angle\boldsymbol{\varphi}_{\rm l}(t) - \left[\frac{\pi}{2}\right] <_t \angle\hat{\boldsymbol{\psi}}(t) <_t \angle\boldsymbol{\varphi}_{\rm r}(t) + \left[\frac{\pi}{2}\right].$$

Fig. 5 illustrates the two cases above and then we can conclude that

(1) If $\theta_{\rm m}(t) = 0$, then $\langle\boldsymbol{\psi}(t), \hat{\boldsymbol{\psi}}(t)\rangle = 0$.
(2) If $0 < \theta_{\rm m}(t) < \pi/2$, then $\langle\boldsymbol{\psi}(t), \hat{\boldsymbol{\psi}}(t)\rangle \le \theta_{\rm m}(t)$.
(3) If $\theta_{\rm m}(t) = \pi/2$, then $\langle\boldsymbol{\psi}(t), \hat{\boldsymbol{\psi}}(t)\rangle < \pi/2$.
(4) If $\pi/2 < \theta_{\rm m}(t) < \pi$, then $\langle\boldsymbol{\psi}(t), \hat{\boldsymbol{\psi}}(t)\rangle < \theta_{\rm m}(t) - \pi/2$.

Therefore, $\langle\boldsymbol{\psi}(t), \hat{\boldsymbol{\psi}}(t)\rangle < \pi/2$ and then $\boldsymbol{\psi}^{\rm T}(t)\hat{\boldsymbol{\psi}}(t) > 0$. Hence, the conclusion of this lemma follows readily.

Then the bounds of $\hat{\rho}_i(t)$ can be given.

Lemma 21. *Suppose Assumptions 17–19 hold. Under the estimators (1) and the control protocol (2), we have $r_{\rm s} \le \hat{\rho}_i(t) \le \rho_i(t)$ for $i = 1, 2, \ldots, n$.*

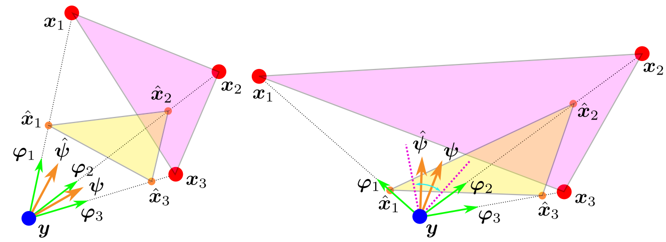

(a) $\theta_{\rm m}(t) \in [0, \frac{\pi}{2})$. (b) $\theta_{\rm m}(t) \in [\frac{\pi}{2}, \pi)$.

Fig. 5. Angle relationship ($n = 3$).

Proof. The proof is divided into 2 steps.

Step 1. In this step, we prove that $\hat{\rho}_i(t) \le \rho_i(t)$. Solving differential equation (5), we have

$$\tilde{\rho}_i(t) = \tilde{\rho}_i(0)e^{-\int_0^t |\omega_i(\tau)|\,\mathrm{d}\tau}. \tag{6}$$

With Assumption 19, we know $\tilde{\rho}_i(0) \le 0$, thus $\tilde{\rho}_i(t) \le 0$ and then $\hat{\rho}_i(t) \le \rho_i(t)$.

Step 2. In this step, we prove that $\hat{\rho}_i(t) \ge r_{\rm s}$. If $\hat{\rho}_i(t) < r_{\rm s}$, then $\hat{D}(t) < \hat{\rho}_i(t) < r_{\rm s}$ and thus $\dot{\boldsymbol{y}}(t) = k[\hat{D}(t) - d]\hat{\boldsymbol{\psi}}(t)$. Considering (4), we have

$$\dot{\hat{\rho}}_i(t) = k[d - \hat{D}(t)]\boldsymbol{\varphi}_i^{\rm T}(t)\hat{\boldsymbol{\psi}}(t) - |v_i(t)|\frac{\tilde{\rho}_i(t)}{\rho_i(t)}.$$

With Assumption 18, $d - \hat{D}(t) > 0$; with Lemma 20, $\boldsymbol{\varphi}_i^{\rm T}(t)\hat{\boldsymbol{\psi}}(t) > 0$; with (6), $-|v_i(t)|\tilde{\rho}_i(t)/\rho_i(t) \ge 0$. Then we know $\dot{\hat{\rho}}_i(t) > 0$ if $\hat{\rho}_i(t) < r_{\rm s}$. Therefore, it follows that $\hat{\rho}_i(t) \ge r_{\rm s}$.

Hence, the conclusion of this lemma follows readily.

The following proposition demonstrates a distance property between two convex hulls which are generated by two closely related point sets. Its proof is in Appendix.

Proposition 22. *Suppose $V = \{\boldsymbol{v}_i\}_{i=1}^m$ is a subset of $\mathbb{S}^1$ and has visual-angle property. Let $P \triangleq \{k_i\boldsymbol{v}_i\}_{i=1}^m$, $Q \triangleq \{l_i\boldsymbol{v}_i\}_{i=1}^m$ be two sets where $k_i, l_i \in \mathbb{R}$, $0 < k_i \le l_i$ for $i = 1, 2, \ldots, m$. Define $P_{\rm c} \triangleq \mathrm{conv}(P)$, $Q_{\rm c} \triangleq \mathrm{conv}(Q)$, $L_P \triangleq \mathrm{dist}(\boldsymbol{0}, P_{\rm c})$ and $L_Q \triangleq \mathrm{dist}(\boldsymbol{0}, Q_{\rm c})$. Then we can assert that $L_P \le L_Q$.*

The relation between $D(t)$ and $\hat{D}(t)$ is revealed below.

Lemma 23. *Suppose Assumptions 17–19 hold. Under the estimators (1) and the control protocol (2), we have $\hat{D}(t) \le D(t)$.*

Proof. It is a direct consequence of Lemma 21 and Proposition 22.

The following proposition reveals the derivative of the distance from a point to a convex set. It is in Hiriart-Urruty and Lemaréchal (1996).

Proposition 24. *Suppose $C \subset \mathbb{R}^2$ is a convex hull of a finite point set. Define a function $f : \mathbb{R}^2 \setminus C \to \mathbb{R}_+, \boldsymbol{a} \mapsto \mathrm{dist}(\boldsymbol{a}, C)$. Let $\boldsymbol{u} \triangleq \mathrm{uv}(\boldsymbol{a}, C)$. Then we can assert that f is differentiable and $\nabla f(\boldsymbol{a}) = -\boldsymbol{u}$.*

With the above proposition, the derivative of $D(t)$ can be calculated as below.

Lemma 25. *If $D(t) > 0$, then $\dot{D}(t) = -\boldsymbol{\psi}^{\rm T}(t)\dot{\boldsymbol{y}}(t)$.*

Proof. If $D(t) > 0$, then $\boldsymbol{\psi}(t)$ is definable. Define a function $f : \mathbb{R}^2 \setminus C \to \mathbb{R}_+, \boldsymbol{a} \mapsto \mathrm{dist}(\boldsymbol{a}, C)$. With Proposition 24, we know $\nabla f(\boldsymbol{y}(t)) = -\boldsymbol{\psi}(t)$. Note that $D(t)$ can be expressed as a

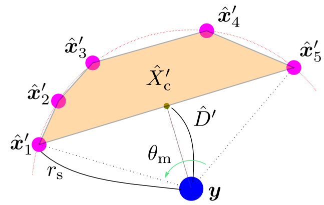

Fig. 6. $\hat{X}'_c(t)$ ($n = 5$).

composite function such that $D = f \circ \boldsymbol{y}$. Using the chain rule, we have $\dot{D}(t) = [\nabla f(\boldsymbol{y}(t))]^{\mathrm{T}}\dot{\boldsymbol{y}}(t) = -\boldsymbol{\psi}^{\mathrm{T}}(t)\dot{\boldsymbol{y}}(t)$. Hence, the conclusion of this lemma follows readily.

Here we prove collision does not happen.

Theorem 26. *Suppose Assumptions 17–19 hold. Under the estimators (1) and the control protocol (2), we have $D(t) \geq r_s$.*

Proof. If $D(t) < r_s$, then with Lemma 23, $\hat{D}(t) \leq D(t) < r_s$. Thus $\dot{\boldsymbol{y}}(t) = k[\hat{D}(t) - d]\hat{\boldsymbol{\psi}}(t)$. With Lemma 25, we have

$$\dot{D}(t) = -\boldsymbol{\psi}^{\mathrm{T}}(t)\dot{\boldsymbol{y}}(t) = k[d - \hat{D}(t)]\boldsymbol{\psi}^{\mathrm{T}}(t)\hat{\boldsymbol{\psi}}(t).$$

With Assumption 18, $d - \hat{D}(t) > 0$ and with Lemma 20, $\boldsymbol{\psi}^{\mathrm{T}}(t)\hat{\boldsymbol{\psi}}(t) > 0$. It implies that $\dot{D}(t) > 0$ if $D(t) < r_s$. With Assumption 17, $D(0) \geq r_s$, then $D(t) \geq r_s$ holds. Hence, the conclusion of this theorem follows readily.

In the sequel, lemmas concerning the bounds of $\hat{D}(t)$ and $D(t)$ are introduced.

Lemma 27. *Suppose Assumptions 17–19 hold. Under the estimators (1) and the control protocol (2), we know $\hat{D}(t)$ has a positive lower bound.*

Proof. Let $\theta_m^* \triangleq \sup_{t\geq 0}\theta_m(t)$. With Theorem 26, we know $D(t) \geq r_s$ for every t, thus $\theta_m^* < \pi$. Let $\hat{\boldsymbol{x}}'_i(t) \triangleq \boldsymbol{y}(t) + r_s\boldsymbol{\varphi}_i(t)$ ($i = 1, 2, \ldots, n$), $\hat{X}'(t) \triangleq \{\hat{\boldsymbol{x}}'_i(t)\}_{i=1}^n$, $\hat{X}'_c(t) \triangleq \mathrm{conv}(\hat{X}'(t))$, $\hat{D}'(t) \triangleq \mathrm{dist}(\boldsymbol{y}(t), \hat{X}'_c(t))$. As is shown in Fig. 6, it follows that $\hat{D}'(t) = r_s\cos(\theta_m(t)/2) \geq r_s\cos(\theta_m^*/2)$. Recall that $\hat{\boldsymbol{x}}_i(t) = \boldsymbol{y}(t) + \hat{\rho}_i(t)\boldsymbol{\varphi}_i(t)$. With Lemma 21, $\hat{\rho}_i(t) \geq r_s$. Then using Proposition 22, we know $\hat{D}(t) \geq \hat{D}'(t) \geq r_s\cos(\theta_m^*/2)$. Hence, the conclusion of this lemma follows readily.

Remark 28. The condition that $D(t)$ and $\hat{D}(t)$ both have positive lower bound ensures that the unit vectors $\boldsymbol{\varphi}_i(t)$, $\bar{\boldsymbol{\varphi}}_i(t)$, $\boldsymbol{\psi}(t)$, $\bar{\boldsymbol{\psi}}(t)$, $\hat{\boldsymbol{\psi}}(t)$, $\hat{\bar{\boldsymbol{\psi}}}(t)$ are definable.

The following proposition considers the property of a set whose point elements are within a distance to a given convex hull. Its proof is in Appendix.

Proposition 29. *Suppose $P = \{\boldsymbol{p}_i\}_{i=1}^m$ is a subset of $\mathbb{R}^2$, $\boldsymbol{a} \in \mathbb{R}^2$ is a point. Let $P_c \triangleq \mathrm{conv}(P)$, $B_s \triangleq \{\boldsymbol{b} \in \mathbb{R}^2 \mid \mathrm{dist}(\boldsymbol{b}, P_c) \leq s\}$ for some $s \geq 0$, $L_P \triangleq \mathrm{dist}(\boldsymbol{a}, P_c)$, $L_B \triangleq \mathrm{dist}(\boldsymbol{a}, B_s)$. Then we can assert that B_s is convex and $L_P \leq L_B + s$.*

Then the boundedness of $D(t)$ can be verified.

Lemma 30. *Suppose Assumptions 17–19 hold. Under the estimators (1) and the control protocol (2), we know $D(t)$ is bounded.*

Proof. With Lemma 25, $\dot{D}(t) = -\boldsymbol{\psi}^{\mathrm{T}}(t)\dot{\boldsymbol{y}}(t) = k[d - \hat{D}(t)]\boldsymbol{\psi}^{\mathrm{T}}(t)\hat{\boldsymbol{\psi}}(t) - \alpha u(\hat{D}(t) - r_s)\boldsymbol{\psi}^{\mathrm{T}}(t)\hat{\bar{\boldsymbol{\psi}}}(t)$. It is easy to conclude that there exists $M > 0$ such that if $D(t) > M$, we have $\theta_m(t) < \pi/3$, thus $\boldsymbol{\psi}^{\mathrm{T}}(t)\hat{\boldsymbol{\psi}}(t) > 1/2$. Let $\tilde{\rho}_0^* \triangleq \max_{1\leq i\leq n}|\tilde{\rho}_i(0)|$. Firstly we verify that $D(t) - \hat{D}(t) \leq \tilde{\rho}_0^*$ for $t \geq 0$. Let $A \triangleq \{\boldsymbol{a} \in \mathbb{R}^2 \mid \mathrm{dist}(\boldsymbol{a}, X_c) \leq \tilde{\rho}_0^*\}$, $L_A(t) \triangleq \mathrm{dist}(\boldsymbol{y}(t), A)$. With Proposition 29, A is convex and $D(t) \leq L_A(t) + \tilde{\rho}_0^*$. Since $\mathrm{dist}(\hat{\boldsymbol{x}}_i(t), X_c) \leq \|\hat{\boldsymbol{x}}_i(t) - \boldsymbol{x}_i\| = |\tilde{\rho}_i(t)| \leq \tilde{\rho}_0^*$, we know $\hat{\boldsymbol{x}}_i(t) \in A$. Thus $\hat{X}_c(t) \subset A$ because A is convex. Considering that $\hat{D}(t) = \mathrm{dist}(\boldsymbol{y}(t), \hat{X}_c(t)) \geq \mathrm{dist}(\boldsymbol{y}(t), A) = L_A(t)$, then we have $D(t) - \hat{D}(t) \leq D(t) - L_A(t) \leq \tilde{\rho}_0^*$. Let $N \triangleq \max\{M, d + \tilde{\rho}_0^* + (2\alpha/k)\}$. If $D(t) \geq N$, then $d - \hat{D}(t) \leq d + \tilde{\rho}_0^* - D(t) \leq -2\alpha/k$, $\boldsymbol{\psi}^{\mathrm{T}}(t)\hat{\boldsymbol{\psi}}(t) > 1/2$. Thus $k[d - \hat{D}(t)]\boldsymbol{\psi}^{\mathrm{T}}(t)\hat{\boldsymbol{\psi}}(t) \leq k \cdot (-2\alpha/k) \cdot (1/2) = -\alpha$. Note that $|\alpha u(\hat{D}(t) - r_s)\boldsymbol{\psi}^{\mathrm{T}}(t)\hat{\bar{\boldsymbol{\psi}}}(t)| \leq \alpha$, then $\dot{D}(t) \leq 0$ if $D(t) \geq N$. Therefore, $D(t)$ is upper-bounded. Hence, the conclusion of this lemma follows readily.

3.2.2. Convex-circumnavigation

With the safety guaranteed, in this subsection, we prove that the agent finally performs convex-circumnavigation around all of the targets.

Firstly, we aim to verify that each estimate must converge. To this end, some lemmas are listed below.

Lemma 31. *Suppose Assumptions 17–19 hold. Under the estimators (1) and the control protocol (2), each $\tilde{\rho}_i(t)$ must converge and $\lim_{t\to+\infty}\tilde{\rho}_i(t) = 0 \Leftrightarrow \int_0^{+\infty}|\omega_i(\tau)|\,\mathrm{d}\tau = +\infty$.*

Proof. Recall (6): $\tilde{\rho}_i(t) = \tilde{\rho}_i(0)\exp\left(-\int_0^t|\omega_i(\tau)|\,\mathrm{d}\tau\right)$. Note that $\tilde{\rho}_i(t)$ is monotone and bounded, thus it must converge. It is obvious that

(1) If $\lim_{t\to+\infty}\tilde{\rho}_i(t) = 0$, then $\int_0^{+\infty}|\omega_i(\tau)|\,\mathrm{d}\tau = +\infty$.
(2) If $\int_0^{+\infty}|\omega_i(\tau)|\,\mathrm{d}\tau = +\infty$, then $\lim_{t\to+\infty}\tilde{\rho}_i(t) = 0$.

Hence, the conclusion of this lemma follows readily.

Lemma 32. *Suppose Assumptions 17–19 hold. Under the estimators (1) and the control protocol (2), if for some i_0, there is $\lim_{t\to+\infty}\tilde{\rho}_{i_0}(t) \neq 0$, then $\boldsymbol{\varphi}_{i_0}(t)$ must converge to some unit vector.*

Proof. Recalling (3), there is $\dot{\boldsymbol{\varphi}}_{i_0}(t) = -\omega_{i_0}(t)\bar{\boldsymbol{\varphi}}_{i_0}(t)$. Let $j = \sqrt{-1}$. Use complex number to represent the vectors, $\varphi_{i_0}(t)$ as $\boldsymbol{\varphi}_{i_0}(t)$ and $-j\varphi_{i_0}(t)$ as $\bar{\boldsymbol{\varphi}}_{i_0}(t)$. Then we obtain $\dot{\varphi}_{i_0}(t) = j\omega_{i_0}(t)\varphi_{i_0}(t)$. Thus we have $\varphi_{i_0}(t) = \varphi_{i_0}(0)\exp\left(j\int_0^t\omega_{i_0}(\tau)\,\mathrm{d}\tau\right)$. From Lemma 31, we know if $\lim_{t\to+\infty}\tilde{\rho}_{i_0}(t) \neq 0$, then $\int_0^{+\infty}|\omega_{i_0}(\tau)|\,\mathrm{d}\tau < +\infty$, and thus $\int_0^{+\infty}\omega_{i_0}(\tau)\,\mathrm{d}\tau$ converges. So $\varphi_{i_0}(t)$ converges, then $\boldsymbol{\varphi}_{i_0}(t)$ converges. Hence, the conclusion of this lemma follows readily.

Now we confirm the convergence of each estimate.

Theorem 33. *Suppose Assumptions 17–19 hold. Under the estimators (1) and the control protocol (2), each $\hat{\boldsymbol{x}}_i(t)$ must converge to some point.*

Proof. Note that

$$\hat{\boldsymbol{x}}_i(t) = \boldsymbol{y}(t) + \hat{\rho}_i(t)\boldsymbol{\varphi}_i(t) = \boldsymbol{x}_i + \tilde{\rho}_i(t)\boldsymbol{\varphi}_i(t). \tag{7}$$

Since with Lemma 31, $\tilde{\rho}_i(t)$ must converge, then we have the following two cases:

(1) If $\lim_{t\to+\infty}\tilde{\rho}_i(t) = 0$, then $\lim_{t\to+\infty}\tilde{\rho}_i(t)\boldsymbol{\varphi}_i(t) = \boldsymbol{0}$ and thus $\hat{\boldsymbol{x}}_i(t)$ converges.
(2) If $\lim_{t\to+\infty}\tilde{\rho}_i(t) \neq 0$, with Lemma 32, we know that $\boldsymbol{\varphi}_i(t)$ converges and thus $\hat{\boldsymbol{x}}_i(t)$ converges.

Hence, the conclusion of this theorem follows readily.

The following proposition reveals a distance relationship between the corresponding points in two convex hulls. Its proof is in Appendix.

Proposition 34. *Suppose $P = \{\boldsymbol{p}_i\}_{i=1}^m$, $Q = \{\boldsymbol{q}_i\}_{i=1}^m$ are two subsets of $\mathbb{R}^2$, $\boldsymbol{a} \in \mathbb{R}^2$ is a point. Let $P_c \triangleq \mathrm{conv}(P)$, $Q_c \triangleq \mathrm{conv}(Q)$, $\boldsymbol{p} \triangleq \mathrm{prj}(\boldsymbol{a}, P_c)$. With Definition 3, there exist $k_i > 0$, $i = 1, 2, \ldots, m$, $\sum_{i=1}^m k_i = 1$ such that $\boldsymbol{p} = \sum_{i=1}^m k_i\boldsymbol{p}_i$. Let $\boldsymbol{p}' \triangleq \sum_{i=1}^m k_i\boldsymbol{q}_i \in Q_c$. If there exists $\varepsilon > 0$ such that $\|\boldsymbol{p}_i - \boldsymbol{q}_i\| < \varepsilon$ for $i = 1, 2, \ldots, m$, then we can assert that $\|\boldsymbol{p} - \boldsymbol{p}'\| < \varepsilon$.*

The below proposition reveals another distance relationship. Its proof is in Appendix.

Proposition 35. *Suppose $P = \{\boldsymbol{p}_i\}_{i=1}^m$ is a subset of $\mathbb{R}^2$. Let $P_c \triangleq \mathrm{conv}(P)$. Suppose $\boldsymbol{a} \in \mathbb{R}^2 \setminus P_c$ is a point. Let $L_P \triangleq \mathrm{dist}(\boldsymbol{a}, P_c)$, $\boldsymbol{p} \triangleq \mathrm{prj}(\boldsymbol{a}, P_c)$. If there is a point $\boldsymbol{b} \in P_c$ such that $\|\boldsymbol{a} - \boldsymbol{b}\| \le L_P + s$, then we can assert that $\|\boldsymbol{b} - \boldsymbol{p}\| \le \sqrt{s^2 + 2sL_P}$.*

In the following theorem, we assert that with the convergence of each estimate, the convex-circumnavigation must be performed around the estimates' limits.

Theorem 36. *Suppose Assumptions 17–19 hold. Under the estimators (1) and the control protocol (2), if there exists a point set $Z = \{\boldsymbol{z}_1, \boldsymbol{z}_2, \ldots, \boldsymbol{z}_n\} \subset \mathbb{R}^2$ such that $\lim_{t\to+\infty} \hat{\boldsymbol{x}}_i(t) = \boldsymbol{z}_i$, then the agent performs convex-circumnavigation around Z with the distance d and the speed α.*

Proof. The proof is divided into 4 steps.

Step 1. Define $Z_c \triangleq \mathrm{conv}(Z)$, $L_Z(t) \triangleq \mathrm{dist}(\boldsymbol{y}(t), Z_c)$. In this step, we prove that

$$\lim_{t\to+\infty} [\hat{D}(t) - L_Z(t)] = 0. \tag{8}$$

For any $\varepsilon_1 > 0$, we know there exists $t_1 > 0$ such that $\|\hat{\boldsymbol{x}}_i(t) - \boldsymbol{z}_i(t)\| < \varepsilon_1$ for $t > t_1$. Let $\boldsymbol{z}(t) \triangleq \mathrm{prj}(\boldsymbol{y}(t), Z_c)$. Then there exist $k_i(t) \ge 0$, $i = 1, 2, \ldots, n$, $\sum_{i=1}^n k_i(t) = 1$ such that $\boldsymbol{z}(t) = \sum_{i=1}^n k_i(t)\boldsymbol{z}_i$. Let $\boldsymbol{z}'(t) \triangleq \sum_{i=1}^n k_i(t)\hat{\boldsymbol{x}}_i(t)$. With Definition 3, $\boldsymbol{z}'(t) \in \hat{X}_c(t)$. With Proposition 34, we know $\|\boldsymbol{z}'(t)-\boldsymbol{z}(t)\| < \varepsilon_1$ for $t > t_1$. Thus, when $t > t_1$, we have $\hat{D}(t) - L_Z(t) \le \|\boldsymbol{y}(t) - \boldsymbol{z}'(t)\| - \|\boldsymbol{y}(t) - \boldsymbol{z}(t)\| \le \|\boldsymbol{z}'(t) - \boldsymbol{z}(t)\| < \varepsilon_1$. Let $\hat{\boldsymbol{x}}(t) \triangleq \mathrm{prj}(\boldsymbol{y}(t), \hat{X}_c(t))$. Then there exist $\hat{k}_i(t) \ge 0$, $i = 1, 2, \ldots, n$, $\sum_{i=1}^n \hat{k}_i(t) = 1$ such that $\hat{\boldsymbol{x}}(t) = \sum_{i=1}^n \hat{k}_i(t)\hat{\boldsymbol{x}}_i(t)$. Let $\hat{\boldsymbol{x}}'(t) \triangleq \sum_{i=1}^n \hat{k}_i(t)\boldsymbol{z}_i$. With Definition 3, $\hat{\boldsymbol{x}}'(t) \in Z_c$. With Proposition 34 again, we know $\|\hat{\boldsymbol{x}}'(t) - \hat{\boldsymbol{x}}(t)\| < \varepsilon_1$ for $t > t_1$. Thus, when $t > t_1$, we have $L_Z(t) - \hat{D}(t) \le \|\boldsymbol{y}(t) - \hat{\boldsymbol{x}}'(t)\| - \|\boldsymbol{y}(t) - \hat{\boldsymbol{x}}(t)\| \le \|\hat{\boldsymbol{x}}'(t) - \hat{\boldsymbol{x}}(t)\| < \varepsilon_1$. Therefore, $|\hat{D}(t) - L_Z(t)| < \varepsilon_1$ for $t > t_1$, which implies that $\lim_{t\to+\infty}[\hat{D}(t) - L_Z(t)] = 0$.

Step 2. In this step, we are going to prove that

$$\lim_{t\to+\infty} [\hat{\boldsymbol{x}}(t) - \boldsymbol{z}(t)] = \boldsymbol{0}. \tag{9}$$

From Lemma 30, we know the movement of the agent is bounded, so $L_Z(t)$ is also bounded. Let $L_Z^* \triangleq \sup_{t\ge 0} L_Z(t)$. Considering (8), for any $\varepsilon_2 \in (0, \sqrt{12L_Z^*})$, there exists $t_2 > 0$ such that $\|\hat{\boldsymbol{x}}_i(t) - \boldsymbol{z}_i(t)\| < \varepsilon_{20}/2$ and $|\hat{D}(t) - L_Z(t)| < \varepsilon_{20}/2$ for $\forall t > t_2$, where $\varepsilon_{20} \triangleq \min\{\varepsilon_2^2/(12L_Z^*), \varepsilon_2/2\} \le L_Z^*$. With Proposition 34, we know $\|\hat{\boldsymbol{x}}(t) - \hat{\boldsymbol{x}}'(t)\| < \varepsilon_{20}/2$. Note that $\|\boldsymbol{y}(t) - \hat{\boldsymbol{x}}'(t)\| \le \|\boldsymbol{y}(t) - \hat{\boldsymbol{x}}(t)\| + \|\hat{\boldsymbol{x}}(t) - \hat{\boldsymbol{x}}'(t)\| = \hat{D}(t) + \|\hat{\boldsymbol{x}}(t) - \hat{\boldsymbol{x}}'(t)\| \le L_Z(t) + |\hat{D}(t) - L_Z(t)| + \|\hat{\boldsymbol{x}}(t) - \hat{\boldsymbol{x}}'(t)\| \le L_Z(t) + \varepsilon_{20}/2 + \varepsilon_{20}/2 = L_Z(t) + \varepsilon_{20}$. Thus, with Proposition 35, one gets $\|\hat{\boldsymbol{x}}'(t) - \boldsymbol{z}(t)\| \le \sqrt{\varepsilon_{20}^2 + 2\varepsilon_{20}L_Z(t)} \le \sqrt{3L_Z^*\varepsilon_{20}} \le \sqrt{3L_Z^*\varepsilon_2^2/(12L_Z^*)} \le \varepsilon_2/2$. Therefore, when $t > t_2$, we have $\|\hat{\boldsymbol{x}}(t) - \boldsymbol{z}(t)\| \le \|\hat{\boldsymbol{x}}(t) - \hat{\boldsymbol{x}}'(t)\| + \|\hat{\boldsymbol{x}}'(t) - \boldsymbol{z}(t)\| \le \varepsilon_2/2 + \varepsilon_2/2 = \varepsilon_2$, which implies that $\lim_{t\to+\infty}[\hat{\boldsymbol{x}}(t) - \boldsymbol{z}(t)] = \boldsymbol{0}$.

Step 3. With Lemma 27 and (8), we know there exists $t_0 > 0$ such that $L_Z(t) > 0$ for $t > t_0$. Then we can define $\boldsymbol{\xi}(t) \triangleq \mathrm{uv}(\boldsymbol{y}(t), Z_c)$ and $\bar{\boldsymbol{\xi}}(t)$ as $\boldsymbol{\xi}(t)$ rotates $\pi/2$ clockwise. In this step, we are supposed to prove that

$$\lim_{t\to+\infty} [\hat{\boldsymbol{\psi}}(t) - \boldsymbol{\xi}(t)] = \boldsymbol{0}, \quad \lim_{t\to+\infty} [\hat{\bar{\boldsymbol{\psi}}}(t) - \bar{\boldsymbol{\xi}}(t)] = \boldsymbol{0}.$$

Let $\hat{D}_* \triangleq \inf_{t\ge 0} D(t)$. With (9), for any $\varepsilon_3 > 0$, there exists $t_3 > t_0$ such that $\|\hat{\boldsymbol{x}}(t) - \boldsymbol{z}(t)\| < \hat{D}_*\varepsilon_3/2$ for $t > t_3$. Therefore, when $t > t_3$, we have ("(t)" is omitted)

$$\begin{aligned}
\|\hat{\boldsymbol{\psi}} - \boldsymbol{\xi}\| &= \left\| \frac{\hat{\boldsymbol{x}} - \boldsymbol{y}}{\|\hat{\boldsymbol{x}} - \boldsymbol{y}\|} - \frac{\boldsymbol{z} - \boldsymbol{y}}{\|\boldsymbol{z} - \boldsymbol{y}\|} \right\| \\
&= \frac{1}{\|\hat{\boldsymbol{x}} - \boldsymbol{y}\|} \left\| [\hat{\boldsymbol{x}} - \boldsymbol{y}] - \frac{\|\hat{\boldsymbol{x}} - \boldsymbol{y}\|}{\|\boldsymbol{z} - \boldsymbol{y}\|}[\boldsymbol{z} - \boldsymbol{y}] \right\| \\
&= \frac{1}{\hat{D}} \left\| [\hat{\boldsymbol{x}} - \boldsymbol{z}] + [\boldsymbol{z} - \boldsymbol{y}] - \frac{\|\hat{\boldsymbol{x}} - \boldsymbol{y}\|}{\|\boldsymbol{z} - \boldsymbol{y}\|}[\boldsymbol{z} - \boldsymbol{y}] \right\| \\
&\le \frac{1}{\hat{D}} \left[\|\hat{\boldsymbol{x}} - \boldsymbol{z}\| \left\| [\boldsymbol{z} - \boldsymbol{y}] - \frac{\|\hat{\boldsymbol{x}} - \boldsymbol{y}\|}{\|\boldsymbol{z} - \boldsymbol{y}\|}[\boldsymbol{z} - \boldsymbol{y}] \right\| \right] \\
&= \frac{\|\hat{\boldsymbol{x}} - \boldsymbol{z}\| + \big| \|\boldsymbol{z} - \boldsymbol{y}\| - \|\hat{\boldsymbol{x}} - \boldsymbol{y}\| \big|}{\hat{D}} \\
&\le \frac{2\|\hat{\boldsymbol{x}} - \boldsymbol{z}\|}{\hat{D}} \le \frac{2}{\hat{D}_*} \cdot \frac{\hat{D}_*}{2}\varepsilon_3 = \varepsilon_3.
\end{aligned}$$

Thus, $\lim_{t\to+\infty}[\hat{\boldsymbol{\psi}}(t) - \boldsymbol{\xi}(t)] = \boldsymbol{0}$. Then obviously $\lim_{t\to+\infty}[\hat{\bar{\boldsymbol{\psi}}}(t) - \bar{\boldsymbol{\xi}}(t)] = \boldsymbol{0}$ holds as well.

Step 4. With the preparations in the previous steps, in this step, we finally prove that

$$\lim_{t\to+\infty} L_Z(t) = d, \quad \lim_{t\to+\infty} \bar{\boldsymbol{\xi}}^{\mathrm{T}}(t)\dot{\boldsymbol{y}}(t) = \alpha,$$

which implies that convex-circumnavigation is performed by the agent around Z with the distance d and the speed α.

Let $e(t) \triangleq L_Z(t) - \hat{D}(t)$, $\boldsymbol{\delta}(t) \triangleq \boldsymbol{\xi}(t) - \hat{\boldsymbol{\psi}}(t)$, $\bar{\boldsymbol{\delta}}(t) \triangleq \bar{\boldsymbol{\xi}}(t) - \hat{\bar{\boldsymbol{\psi}}}(t)$. With Step 1 and 3, we know $\lim_{t\to+\infty} e(t) = 0$, $\lim_{t\to+\infty} \boldsymbol{\delta}(t) = \lim_{t\to+\infty} \bar{\boldsymbol{\delta}}(t) = \boldsymbol{0}$. Similar to Lemma 25, we can conclude that $\dot{L}_Z(t) = -\boldsymbol{\xi}^{\mathrm{T}}(t)\dot{\boldsymbol{y}}(t) = k[d - \hat{D}(t)]\boldsymbol{\xi}^{\mathrm{T}}(t)\hat{\boldsymbol{\psi}}(t) - \alpha u(\hat{D}(t) - r_s)\boldsymbol{\xi}^{\mathrm{T}}(t)\hat{\bar{\boldsymbol{\psi}}}(t) = -kL_Z(t) + kd + g(t)$, where $g(t) \triangleq ke(t) + k[d - \hat{D}(t)]\boldsymbol{\delta}^{\mathrm{T}}(t)\hat{\boldsymbol{\psi}}(t) - \alpha u(\hat{D}(t) - r_s)\boldsymbol{\delta}^{\mathrm{T}}(t)\hat{\bar{\boldsymbol{\psi}}}(t)$. Since $\lim_{t\to+\infty} g(t) = 0$, we have $\lim_{t\to+\infty} L_Z(t) = d$. Note that $\bar{\boldsymbol{\xi}}^{\mathrm{T}}(t)\dot{\boldsymbol{y}}(t) = k[\hat{D}(t) - d]\bar{\boldsymbol{\xi}}^{\mathrm{T}}(t)\hat{\boldsymbol{\psi}}(t) + \alpha u(\hat{D}(t) - r_s)\bar{\boldsymbol{\xi}}^{\mathrm{T}}(t)\hat{\bar{\boldsymbol{\psi}}}(t) = \alpha u(\hat{D}(t) - r_s) + h(t)$, where $h(t) \triangleq k[\hat{D}(t) - d]\bar{\boldsymbol{\delta}}^{\mathrm{T}}(t)\hat{\boldsymbol{\psi}}(t) + \alpha u(\hat{D}(t) - r_s)\bar{\boldsymbol{\delta}}^{\mathrm{T}}(t)\hat{\bar{\boldsymbol{\psi}}}(t)$. With (8), we know $\lim_{t\to+\infty} \hat{D}(t) = \lim_{t\to+\infty} L_Z(t) = d$. Recall Assumption 18 that $d > r_s$. Then there exists $t_4 > 0$ such that $\hat{D}(t) > r_s$ for $t > t_4$. Therefore, when $t > t_4$, $u(\hat{D}(t) - r_s) = 1$, and then one gets $\bar{\boldsymbol{\xi}}^{\mathrm{T}}(t)\dot{\boldsymbol{y}}(t) = \alpha + h(t)$. With $\lim_{t\to+\infty} h(t) = 0$, we have $\lim_{t\to+\infty} \bar{\boldsymbol{\xi}}^{\mathrm{T}}(t)\dot{\boldsymbol{y}}(t) = \alpha$.

Hence, the conclusion of this theorem follows readily.

Until now, we have already concluded that the agent performs convex-circumnavigation around some area eventually. But it is still uncertain whether this area is the convex hull of all of the targets. The next two theorems confirm that the targets are exactly located in the end and ensure that "this area" is exactly the convex hull of all the targets.

Theorem 37. *Suppose Assumptions 17–19 hold. Under the estimators (1) and the control protocol (2), localization of all of the targets is achieved.*

Proof. Apply the reduction to absurdity. Suppose for some i_0, there is $\lim_{t\to+\infty} \tilde{\rho}_i(t) \ne 0$. Then with Lemma 32, $\boldsymbol{\varphi}_{i_0}(t)$ converges. With Theorem 33 and 36, we know that the agent must finally perform convex-circumnavigation around some points.

Table 1
Simulation configuration.

$\boldsymbol{y}(0)$		k	d	α	r_s
$[8, 0]^{\mathrm{T}}$ m		1	0.5 m	5 m/s	0.3 m
$\boldsymbol{x}_1$	$[-2, 0]^{\mathrm{T}}$ m	$\hat{\rho}_1(0)$	0.3 m	$\hat{\boldsymbol{x}}_1(0)$	$[7.7, 0]^{\mathrm{T}}$ m
$\boldsymbol{x}_2$	$[4, 5]^{\mathrm{T}}$ m	$\hat{\rho}_2(0)$	0.3 m	$\hat{\boldsymbol{x}}_2(0)$	$[7.812, 0.234]^{\mathrm{T}}$ m
$\boldsymbol{x}_3$	$[2, 0]^{\mathrm{T}}$ m	$\hat{\rho}_3(0)$	0.3 m	$\hat{\boldsymbol{x}}_3(0)$	$[7.7, 0]^{\mathrm{T}}$ m
$\boldsymbol{x}_4$	$[1, 1]^{\mathrm{T}}$ m	$\hat{\rho}_4(0)$	0.3 m	$\hat{\boldsymbol{x}}_4(0)$	$[7.703, 0.042]^{\mathrm{T}}$ m

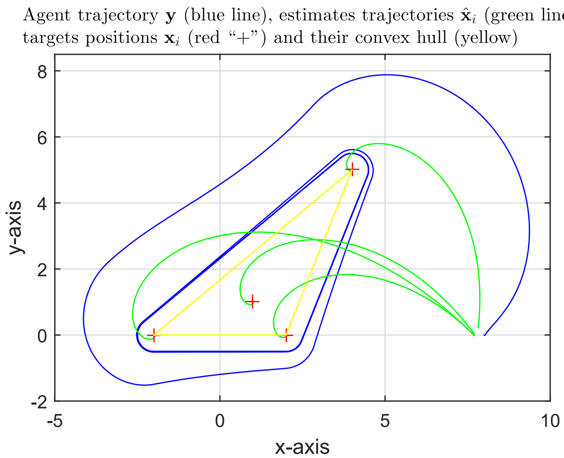

Fig. 7. Trajectories in X–Y plane. (For interpretation of the references to color in this figure legend, the reader is referred to the web version of this article.)

Thus, for any i, $\boldsymbol{\varphi}_i(t)$ will not converge. Contradiction appears. Hence, the conclusion of this theorem follows readily.

Theorem 38. *Suppose Assumptions 17–19 hold. Under the estimators (1) and the control protocol (2), the agent performs safe convex-circumnavigation around all of the targets with the distance d and the speed α.*

Proof. Recall (7): $\hat{\boldsymbol{x}}_i(t) = \boldsymbol{x}_i + \tilde{\rho}_i(t)\boldsymbol{\varphi}_i(t)$. With Theorem 37, $\lim_{t\to+\infty} \tilde{\rho}_i(t) = 0$, thus we have $\lim_{t\to+\infty} \hat{\boldsymbol{x}}_i(t) = \boldsymbol{x}_i$. With Theorem 36, the agent performs convex-circumnavigation around X with the distance d and the speed α. With Theorem 26, the circumnavigation meets the safety requirement. Hence, the conclusion of this theorem follows readily.

4. Simulations

In this section, MATLAB simulation results for the safe convex-circumnavigation are presented. The two simulations share a common configuration (see Table 1). One is without noise and another one is with noise. Figs. 7–9 show the results of the simulation without noise. It is shown in Fig. 7 that the agent encloses the convex hull of all of the targets with the expected radius. Green lines show that each target's estimate $\hat{\boldsymbol{x}}_i(t)$ converges to the real target $\boldsymbol{x}_i$. Fig. 8 depicts the image of the distance $D(t)$ from the agent to the convex hull of all the targets and shows that $D(t)$ converges to the expected encircling distance d finally. Fig. 9 depicts the image of $\bar{\boldsymbol{\psi}}^{\mathrm{T}}(t)\dot{\boldsymbol{y}}(t)$ and shows that the agent's lateral speed relative to the convex hull of all the targets converges to the desired speed α. Collision does not happen in the whole circumnavigation process. Therefore, from this simulation, it is concluded that the agent circumnavigates the convex hull of the targets' estimates and the safe convex-circumnavigation is achieved with the convergence of the estimators. In the simulation with noise, gaussian noises are added into the positions of the targets.The noise is $n(\cdot)$ (m) such that $\mathrm{E}[n(t)] = 0$ m and $\mathrm{E}[n(t)n(s)] = 0.01\delta(t-s)$ m^2. Results are shown in Figs. 10–12. Circumnavigation is performed well even in the presence of noise.

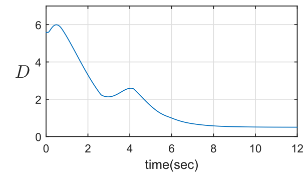

Fig. 8. Distance between the agent and the targets' convex hull.

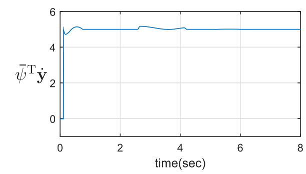

Fig. 9. Lateral speed relative to the targets' convex hull.

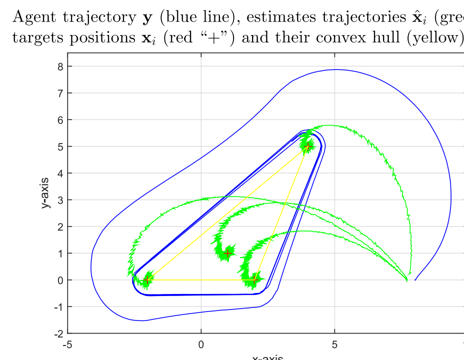

Fig. 10. Trajectories in X-Y plane with noise.

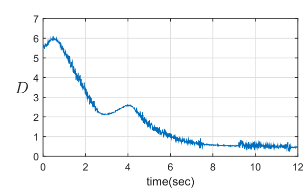

Fig. 11. Distance between the agent and the targets' convex hull with noise.

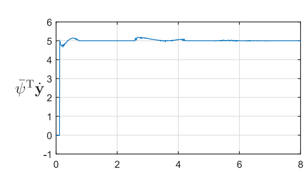

Fig. 12. Lateral speed relative to the targets' convex hull with noise.

5. Discussion about moving targets

In this section, the case with moving targets is discussed and a conjecture is proposed, which is validated via an experiment.

5.1. Analysis

Conjecture 39. *If the targets move and their speeds $\|\dot{\boldsymbol{x}}_i(t)\|$ are bounded, then $D(t)$ converges to a neighborhood of zero.*

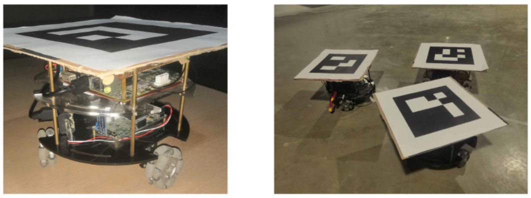

(a) Agent. (b) Targets.

Fig. 13. Experimental platform.

Rationale. For $i = 1, 2, \ldots, n$, let $u_i(t) \triangleq \boldsymbol{\varphi}_i^{\mathrm{T}}(t)\dot{\boldsymbol{x}}_i(t)$, $\bar{u}_i(t) \triangleq \mathrm{sgn}(\bar{v}_i)\bar{\boldsymbol{\varphi}}_i^{\mathrm{T}}(t)\dot{\boldsymbol{x}}_i(t)$. Then we have

$$
\begin{aligned}
\dot{\rho}_i &= u_i - v_i,\\
\dot{\hat{\rho}}_i &= \frac{-|\bar{v}_i| + \bar{u}_i}{\rho_i}\hat{\rho}_i - v_i + |\bar{v}_i|,\\
\dot{\tilde{\rho}}_i &= \frac{-|\bar{v}_i| + \bar{u}_i}{\rho_i}\tilde{\rho}_i - u_i + \bar{u}_i.
\end{aligned}
\tag{10}
$$

Eq. (10) can be viewed as a combination of a nominal system $\dot{z} = \frac{-|\bar{v}_i|+\bar{u}_i}{\rho_i} z$ (suppose the state is $z(t)$), and a bounded perturbation $-u_i + \bar{u}_i$. The solution of the nominal system is $z(t) = z(0)\exp\left(\int_0^t \frac{-|\bar{v}_i(\tau)|+\bar{u}_i(\tau)}{\rho_i(\tau)}\,\mathrm{d}\tau\right)$. Then we can conclude that, if $z(t)$ converges to zero, then $\tilde{\rho}_i(t)$ is bounded and thus $D(t)$ is also bounded.

Remark 40. The convergence property of $z(t)$ is closely related to the term $(-|\bar{v}_i(\tau)| + \bar{u}_i(\tau))/\rho_i(\tau)$. The property of this term is important because the movement of the agent is related to all the targets. To figure out the property this term may be a challenging problem which deserves deeply investigation in the future.

To verify our conjecture, an experiment is done to show the performance of our algorithm in moving targets case.

5.2. Experiment

As for hardware, an omni wheeled robot equipped with an onboard computer (NVIDIA Jetson TK1) is used as the agent (Fig. 13(a)). Another three omni wheel robots are used as targets (Fig. 13(b)). A ceiling camera and ArUco markers are used for the localization of the agent and the targets. We use the software Robot Operating System (ROS) for communication. The configuration of this experiment is: $k = 0.5$, $d = 0.6$ m, $\alpha = 0.6$ m/s, $r_s = 0.4$ m. The experimental result[1] from the camera and RViz (a 3D visualization tool for ROS) is shown in Fig. 14. The experimental results show that the agent can perform convex circumnavigation well even in the moving targets case. In the experiment, we find that each $\tilde{\rho}_i(t)$ keeps small thus collision is unlikely to happen.

6. Conclusions and future works

In this paper, a new kind of circumnavigation — safe convex-circumnavigation is proposed and an algorithm is developed to achieve it using only the agent position and the bearing angles to the targets. We have improved the scalar estimation method in Cao et al. (2020) to locate the targets and designed a control protocol to force the agent to circumnavigate the convex hull of them with a desired distance and speed. Collision is avoided in the whole circumnavigation process. Our result shows that the scalar estimation idea is useful for collision avoidance research and can be extended to multi-target case.

In the future, we plan to apply the scalar estimator to more general problems such as circumnavigating an arbitrary compact convex set. More future works include improving this algorithm to fit in moving targets and multiple agents scenarios as well as developing estimators with a stronger anti-disturbance capacity. Further examination and exploration on system convergence/stability (i.e., input-to-state stability, finite time stability) is also a meaningful topic for future research.

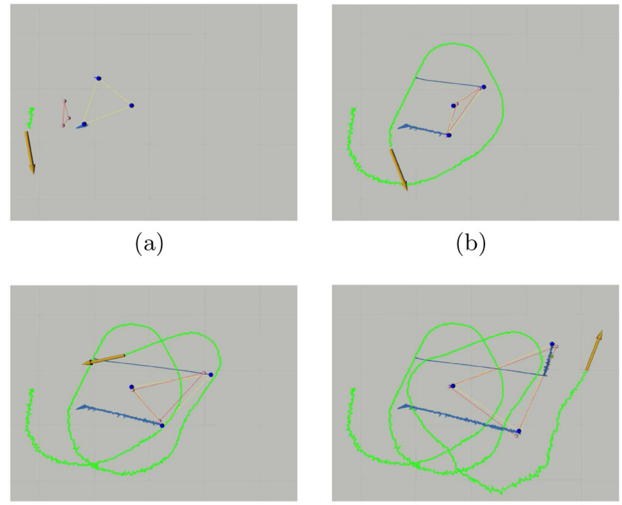

(a) (b) (c) (d)

Fig. 14. Experimental results in RViz. (Here, blue points are targets; blue lines are the trajectories of the targets; pink points are targets' estimates; yellow and red triangles are the convex hulls of the targets and the targets' estimates, respectively; little green point is the projective point from the agent to the convex hull of the targets' estimates; green line is the trajectory of the agent; brown arrow is the velocity of the agent; a grid represents 1 m.). (For interpretation of the references to color in this figure legend, the reader is referred to the web version of this article.)

Appendix

Proof of Proposition 9. $\angle \boldsymbol{v}_{\mathrm{r}} \le \angle \boldsymbol{u} \le \angle \boldsymbol{v}_{\mathrm{l}}$ holds obviously, so we only prove $\langle \boldsymbol{u}, \boldsymbol{v}_i \rangle < \pi/2$ for $i = 1, 2, \ldots, m$. The proof is divided into 2 steps.

Step 1. Let $\boldsymbol{p} \triangleq \mathrm{prj}(\boldsymbol{a}, P_{\mathrm{c}})$. Define a half-plane $H \triangleq \{\boldsymbol{h} \in \mathbb{R}^2 \mid \boldsymbol{u}^{\mathrm{T}}(\boldsymbol{h}-\boldsymbol{p}) \ge 0\}$. Then we prove that $P_{\mathrm{c}} \subset H$. Apply the reduction to absurdity. Suppose $\boldsymbol{b} \in P_{\mathrm{c}} \setminus H$. Let $\lambda \triangleq 2(\boldsymbol{a}-\boldsymbol{p})^{\mathrm{T}}(\boldsymbol{b}-\boldsymbol{p})/\|\boldsymbol{b}-\boldsymbol{p}\|^2 > 0$, $\boldsymbol{c} \triangleq \lambda\boldsymbol{b} + (1-\lambda)\boldsymbol{p}$. Since $\boldsymbol{b} \in P_{\mathrm{c}}$, we know $\|\boldsymbol{a}-\boldsymbol{p}\| < \|\boldsymbol{a}-\boldsymbol{b}\|$. Considering that $\|\boldsymbol{b}-\boldsymbol{p}\|^2(1-\lambda) = \|\boldsymbol{a}-\boldsymbol{b}\|^2 - \|\boldsymbol{a}-\boldsymbol{p}\|^2 > 0$, we have $0 < \lambda < 1$ and thus $\boldsymbol{c} \in P_{\mathrm{c}}$. Then we know $\|\boldsymbol{a}-\boldsymbol{c}\| = \|\boldsymbol{a}-\boldsymbol{p}\|$. With Proposition 4, contradiction appears because $\boldsymbol{p}$ is not the unique minimum distance point of P_{c} to $\boldsymbol{a}$.

Step 2. Suppose $\boldsymbol{d} \in H$. Let $\boldsymbol{v} \triangleq (\boldsymbol{d}-\boldsymbol{a})/\|\boldsymbol{d}-\boldsymbol{a}\|$. It is obvious that $\langle \boldsymbol{u}, \boldsymbol{v} \rangle < \pi/2$. Since $P_{\mathrm{c}} \in H$, we know $\langle \boldsymbol{u}, \boldsymbol{v}_i \rangle < \pi/2$ for $i = 1, 2, \ldots, m$.

Hence, the conclusion of this proposition follows readily.

Proof of Proposition 22. It suffices to prove that for each point $\boldsymbol{q} \in Q_{\mathrm{c}}$, there exists a point $\boldsymbol{p} \in P_{\mathrm{c}}$ such that $\|\boldsymbol{p}\| \le \|\boldsymbol{q}\|$. Suppose $\boldsymbol{q} = \sum_{i=1}^m \mu_i l_i \boldsymbol{v}_i$, $\sum_{i=1}^m \mu_i = 1$. Let $\lambda_i \triangleq (\mu_i l_i/k_i)/(\sum_{j=1}^m \mu_j l_j/k_j)$, $\boldsymbol{p} \triangleq \sum_{i=1}^m \lambda_i k_i \boldsymbol{v}_i$. We know $0 \le \lambda_i \le 1$, $\sum_{i=1}^m \lambda_i = 1$, so $\boldsymbol{p} \in P_{\mathrm{c}}$. Noting that $\sum_{j=1}^m \mu_j l_j/k_j \ge 1$, then $\|\boldsymbol{p}\| = \left\|\boldsymbol{q}/(\sum_{j=1}^m \mu_j l_j/k_j)\right\| =$

[1] The experimental result video is on website https://github.com/shidacao/scc_vedio.

$\|\boldsymbol{q}\|/\left(\sum_{j=1}^{m}\mu_j l_j/k_j\right) \le \|\boldsymbol{q}\|$. Hence, the conclusion of this proposition follows readily.

Proof of Proposition 29. The proof contains 2 steps.

Step 1. In this step, we prove B_s is convex. Suppose there are two points $\boldsymbol{b}_0, \boldsymbol{b}_1 \in B_s$. With the definition of B_s, we know $\mathrm{dist}(\boldsymbol{b}_0, P_c) \le s$ and $\mathrm{dist}(\boldsymbol{b}_1, P_c) \le s$, thus there exist two points $\boldsymbol{p}_0, \boldsymbol{p}_1 \in P_c$ such that $\|\boldsymbol{b}_0 - \boldsymbol{p}_0\| \le s$ and $\|\boldsymbol{b}_1 - \boldsymbol{p}_1\| \le s$. For any $\lambda \in [0, 1]$, let $\boldsymbol{b}_\lambda \triangleq (1-\lambda)\boldsymbol{b}_0 + \lambda\boldsymbol{b}_1$, $\boldsymbol{p}_\lambda \triangleq (1-\lambda)\boldsymbol{p}_0 + \lambda\boldsymbol{p}_1$. Since P_c is convex, we know $\boldsymbol{p}_\lambda \in P_c$. Note that $\|\boldsymbol{b}_\lambda - \boldsymbol{p}_\lambda\| = \left\|[(1-\lambda)\boldsymbol{b}_0 + \lambda\boldsymbol{b}_1] - [(1-\lambda)\boldsymbol{p}_0 + \lambda\boldsymbol{p}_1]\right\| = \| (1-\lambda)(\boldsymbol{b}_0 - \boldsymbol{p}_0) + \lambda(\boldsymbol{b}_1 - \boldsymbol{p}_1) \| \le (1-\lambda)\left\|\boldsymbol{b}_0 - \boldsymbol{p}_0\right\| + \lambda\|\boldsymbol{b}_1 - \boldsymbol{p}_1\| \le (1-\lambda)\cdot s + \lambda\cdot s = s$. Therefore, $\boldsymbol{b}_\lambda \in B_s$ and then B_s is convex.

Step 2. In this step, we prove $L_P \le L_B + s$. Since the function $f(\boldsymbol{c}) = \mathrm{dist}(\boldsymbol{c}, P_c)$ is continuous, the set $B_s = f^{-1}([0, s])$ is closed. Obviously, B_s is bounded, thus B_s is compact. By Proposition 4, there exists a point $\boldsymbol{b}_2 \in B_s$ such that $L_B = \|\boldsymbol{a} - \boldsymbol{b}_2\|$. With the definition of B_s, there exists a point $\boldsymbol{p}_2 \in P_c$ such that $\|\boldsymbol{b}_2 - \boldsymbol{p}_2\| \le s$. Therefore, $L_P \le \|\boldsymbol{a} - \boldsymbol{p}_2\| \le \|\boldsymbol{a} - \boldsymbol{b}_2\| + \|\boldsymbol{b}_2 - \boldsymbol{p}_2\| \le L_B + s$.

Hence, the conclusion of this proposition follows readily.

Proof of Proposition 34. Note that $\|\boldsymbol{p} - \boldsymbol{p}'\| = \left\|\sum_{i=1}^{m} k_i\boldsymbol{p}_i - \sum_{i=1}^{m} k_i\boldsymbol{q}_i\right\| = \left\|\sum_{i=1}^{m} k_i(\boldsymbol{p}_i - \boldsymbol{q}_i)\right\| \le \sum_{i=1}^{m} k_i\|\boldsymbol{p}_i - \boldsymbol{q}_i\| < \sum_{i=1}^{m} k_i\varepsilon = \varepsilon$. Hence, the conclusion of this proposition follows readily.

Proof of Proposition 35. Define half-plane $H \triangleq \{\boldsymbol{h} \in \mathbb{R}^2 \mid (\boldsymbol{p} - \boldsymbol{a})^{\mathrm{T}}(\boldsymbol{h} - \boldsymbol{p}) \ge 0\}$ and circle $S \triangleq \{\boldsymbol{s} \in \mathbb{R}^2 \mid \|\boldsymbol{s} - \boldsymbol{a}\| \le L_P + s\}$. As is shown in Step 1 of the proof of Proposition 9, we know $\boldsymbol{b} \in H$, so $\boldsymbol{b} \in H \cap S$. Let $\boldsymbol{c} \in \mathbb{R}^2$ be one point satisfies $(\boldsymbol{p} - \boldsymbol{a})^{\mathrm{T}}(\boldsymbol{c} - \boldsymbol{p}) = 0$ and $\|\boldsymbol{c} - \boldsymbol{a}\| = L_P + s$. Obviously we have $\|\boldsymbol{b} - \boldsymbol{p}\| \le \|\boldsymbol{c} - \boldsymbol{p}\| = \sqrt{s^2 + 2sL_P}$. Hence, the conclusion of this proposition follows readily.

References

Boyd, S., & Vandenberghe, L. (2004). *Convex optimization*. Cambridge University Press.

Cao, Y. (2014). UAV circumnavigating an unknown target using range measurement and estimated range rate. In *2014 american control conference*, Portland, Oregon, USA (pp. 4581–4586).

Cao, Y. (2015). UAV circumnavigating an unknown target under a GPS-denied environment with range-only measurements. *Automatica*, *55*, 150–158.

Cao, S., Li, R., Shi, Y., & Song, Y. (2020). A low-cost estimator for target localization and circumnavigation using bearing measurements. *Journal of the Franklin Institute*, *357*, 9654–9672.

Chun, S., & Tian, Y.-P. (2020). Multi-targets localization and elliptical circumnavigation by multi-agents using bearing-only measurements in two-dimensional space. *International Journal of Robust and Nonlinear Control*, *30*, 3250–3268.

Deghat, M., Davis, E., See, T., Shames, I., Anderson, B. D. O., & Yu, C. (2012). Target localization and circumnavigation by a non-holonomic robot. In *2012 ieee/rsj international conference on intelligent robots and systems*, Vilamoura, Algarve, Portugal (pp. 1227–1232).

Deghat, M., Shames, I., Anderson, B. D. O., & Yu, C. (2010). Target localization and circumnavigation using bearing measurements in 2D. In *49th ieee conference on decision and control*, Hilton Atlanta Hotel, Atlanta, GA, USA (pp. 334–339).

Deghat, M., Shames, I., Anderson, B. D. O., & Yu, C. (2014). Localization and circumnavigation of a slowly moving target using bearing measurements. *IEEE Transactions on Automatic Control*, *59*(8), 2182–2188.

Deghat, M., Xia, L., Anderson, B. D. O., & Hong, Y. (2015). Multi-target localization and circumnavigation by a single agent using bearing measurements. *International Journal of Robust and Nonlinear Control*, *25*, 2362–2374.

Dou, L., Song, C., Wang, X., Liu, L., & Feng, G. (2020). Target localization and enclosing control for networked mobile agents with bearing measurements. *Automatica*, *118*, Article 109022.

Franchi, A., Stegagno, P., & Oriolo, G. (2016). Decentralized multi-robot encirclement of a 3D target with guaranteed collision avoidance. *Autonomous Robots*, *40*(2), 245–265.

Hashemi, A., Cao, Y., Casbeer, D. W., & Yin, G. (2014). Unmanned aerial vehicle circumnavigation using noisy range-based measurements without global positioning system information. *Journal of Dynamic Systems, Measurement, and Control*, *137*(3), Article 031003.

Hiriart-Urruty, J.-B., & Lemaréchal, C. (1996). *Convex analysis and minimization algorithms i fundamentals*. Springer-Verlag.

Kim, T.-H., & Sugie, T. (2007). Cooperative control for target-capturing task based on a cyclic pursuit strategy. *Automatica*, *43*, 1426–1431.

Lan, Y., Yan, G., & Lin, Z. (2010). Distributed control of cooperative target enclosing based on reachability and invariance analysis. *Systems & Control Letters*, *59*(7), 381–389.

Li, R., Shi, Y., & Song, Y. (2016). Multi-group coordination control of multi-agent system based on smoothing estimator. *IET Control Theory & Applications*, *10*(11), 1224–1230.

Li, R., Shi, Y. J., & Song, Y. D. (2018). Localization and circumnavigation of multiple agents along an unknown target based on bearing-only measurement: A three dimensional solution. *Automatica*, *94*, 18–25.

Li, R., Shi, Y. J., Wu, X. Q., & Song, Y. D. (2019). Safe-circumnavigation of one single agent around a group of targets with only bearing information. *Journal of the Franklin Institute*, *356*, 11546–11560.

Matveev, A. S., & Semakova, A. A. (2017). Localization and three-dimentional circumnavigation of many mobile targets based on distance measurements. *IFAC-PapersOnLine*, *50*(1), 8832–8837.

Matveev, A. S., Semakova, A. A., & Savkin, A. V. (2016). Range-only based circumnavigation of a group of moving targets by a non-holonomic mobile robot. *Automatica*, *65*, 76–89.

Miao, Z., Wang, Y., & Fierro, R. (2017). Cooperative circumnavigation of a moving target with multiple nonholonomic robots using backstepping design. *Systems & Control Letters*, *103*, 58–65.

Milutinović, D., Casbeer, D., Cao, Y., & Kingston, D. (2017). Coordinate frame free dubins vehicle circumnavigation using only range-based measurements. *International Journal of Robust and Nonlinear Control*, *27*(16), 2937–2960.

Qi, G.-Q., Li, Y.-Y., & Sheng, A.-D. (2019). Virtual intersecting location based UAV circumnavigation and bearings-only target-tracking techniques. *Information Sciences*, *505*, 571–585.

Shames, I., Dasgupta, S., Fidan, B., & Anderson, B. D. O. (2012). Circumnavigation using distance measurements under slow drift. *IEEE Transactions on Automatic Control*, *57*(4), 889–903.

Shames, I., Fidan, B., & Anderson, B. D. O. (2011). Close target reconnaissance with guaranteed collision avoidance. *International Journal of Robust and Nonlinear Control*, *21*(16), 1823–1840.

Shao, J., & Tian, Y.-P. (2018). Multi-target localisation and circumnavigation by a multi-agent system with bearing measurements in 2D space. *International Journal of Systems Science*, *49*(1), 15–26.

Shi, Y. J., Li, R., & Teo, K. L. (2015). Cooperative enclosing control for multiple moving targets by a group of agents. *International Journal of Control*, *88*(1), 80–89.

Yu, Y., Li, Z., Wang, X., & Shen, L. (2019). Bearing-only circumnavigation control of the multi-agent system around a moving target. *International Journal of Systems Science*, *13*(17), 2747–2757.

Zheng, R., Liu, Y., & Sun, D. (2015). Enclosing a target by nonholonomic mobile robots with bearing-only measurements. *Automatica*, *53*, 400–407.

Shida Cao received the B.Eng. degree in Automation and the M.Eng. degree in Control Engineering from School of Automation Engineering, University of Electronic Science and Technology of China, Chengdu, China, in 2018 and 2021 respectively. He is going to be a Ph.D. candidate in Control Science and Engineering with School of Astronautics, Harbin Institute of Technology, Harbin, China, in 2021. His research interests focus on coordination control of multi-agent systems.

Rui Li received the Ph.D. degree in Control Science and Engineering from Harbin Institute of Technology, China, in 2008. She joined University of Electronic Science and Technology of China in 2008. She is currently a professor in School of Automation Engineering, University of Electronic Science and Technology of China. Previously, she worked as a Visiting Research Associate with Department of Applied Mathematics, the Hong Kong Polytechnic University for half a year and as Visiting Research Associate with the Department of Mathematics & Statistics, Curtin University of Technology for one year. From September 2011 to September 2012, she was a visiting scholar with Department of Electrical Engineering, University of California at Riverside. Her research interests include multi-agent systems, optimal control, nonlinear control and aircraft control.

Yingjing Shi received the Ph.D. degree from Harbin Institute of Technology, China, in 2008. He has been with University of Electronic Science and Technology of China since 2008. Currently, he is an associate professor with School of Automation Engineering, University of Electronic Science and Technology of China. From August 2013 to August 2014, he was a visiting scholar with the Department of Mathematics & Statistics, Curtin University of Technology. His research interests include aircraft control, multi-agent systems and robust control.

Yongduan Song (Fellow, IEEE) received the Ph. D. degree in electrical and computer engineering from Tennessee Technological University, Cookeville, TN, USA, in 1992. He held a tenured Full Professor with North Carolina A&T State University, Greensboro, NC, USA, from 1993 to 2008, and a Langley Distinguished Professor with the National Institute of Aerospace, Hampton, VA, USA, from 2005 to 2008. He is currently the Dean of the School of Automation, Chongqing University, Chongqing, China. He was one of the six Langley Distinguished Professors with the National Institute of Aerospace (NIA), Hampton, VA, USA, where he was the Founding Director of Cooperative Systems. His current research interests include intelligent systems, guidance navigation and control, and bioinspired adaptive and cooperative systems.

Dr. Song was a recipient of several competitive research awards from the National Science Foundation, the National Aeronautics and Space Administration, the U.S. Air Force Office, the U.S. Army Research Office, and the U.S. Naval Research Office. He is an IEEE Fellow and has served/been serving as an Associate Editor for several prestigious international journals, including the IEEE TRANSACTIONS ON AUTOMATIC CONTROL, the IEEE TRANSACTIONS ON NEURAL NETWORKS AND LEARNING SYSTEMS, the IEEE TRANSACTIONS ON INTELLIGENT TRANSPORTATION SYSTEMS, the IEEE TRANSACTIONS ON SYSTEMS, MAN AND CYBERNETICS, and the IEEE TRANSACTIONS ON DEVELOPMENTAL AND COGNITIVE SYSTEMS. Dr. Song is the Editor-in-Chief Elect for IEEE Trans. on Neural Networks and Learning Systems, assuming his EIC responsibilities starting January 1, 2022.